Chinese Journal of
POLYMER SCIENCE

RESEARCH ARTICLE

https://doi.org/10.1007/s10118-024-3219-0
Chinese J. Polym. Sci. **2024**, *42*, 1976–1985

Viscoelastic Property Evolution of Thermoplastic Polyurethane During Annealing Treatment and Its Correlation with Segmental Crystallization

Jian-Wen Shan[a], Yan-Bo Zhu[b], Ling-Ling Ni[a*], and Peng-Ju Pan[a*]

[a] *State Key Laboratory of Chemical Engineering, College of Chemical and Biological Engineering, Zhejiang University, Hangzhou 310058, China*
[b] *Department of Polymer Science and Engineering, Zhejiang University, Hangzhou 310058, China*

Electronic Supplementary Information

Abstract Viscoelastic properties of thermoplastic polyurethane (TPU) is of fundamental importance for its processing. In this work, we prepared different TPUs from polycaprolactone (PCL) diol, diphenylmethane-4,4′-diisocyanate (MDI), and 1,4-butanediol (BDO), and investigated the viscoelastic behavior of three TPUs with different hard segment content during thermal annealing process. The storage modulus (G') of TPU increases over time in a medium annealing temperature (T_a) region, but remains unchanged at both high and low temperature regions. The growth of loss modulus (G'') over time is slower than that of G'. At medium T_a, both G' and G'' increase during the repeating frequency (ω) sweep, due to the gradual crystallization of hard segments. This indicates that the crystallites primarily restrain the relaxation of unit with large size. The increments of G' and G'' are weakened when the content of hard segment in TPU is decreased. For TPU with high content of hard segments, a complete high elastic platform with a width of 3 orders of magnitude was observed only through one frequency scan test at medium T_a. In addition, the crystallites of hard segments grow up continuously during frequency scan test (isothermal annealing treatment) and cause the extreme increase in G' and G'' with ω in low ω region.

Keywords Thermoplastic polyurethane; Viscoelastic properties; Annealing; Crystallization

Citation: Shan, J. W.; Zhu, Y. B.; Ni, L. L.; Pan, P. J. Viscoelastic property evolution of thermoplastic polyurethane during annealing treatment and its correlation with segmental crystallization. *Chinese J. Polym. Sci.* **2024**, *42*, 1976–1985.

INTRODUCTION

Thermoplastic polyurethane (TPU) has received considerable attention from both the scientific and industrial communities in the last decades.[1–3] TPUs are widely applied in sealing components, shock absorbers, creative toys, artificial hearts, diaphragms, and so on.[4–8] TPUs are linear and multi-block polymers composed of substituting hard and soft segments.[9,10] The hard segments of TPUs are typically composed of diisocyanate [*e.g.*, 4,4′-diphenylmethane diisocyanate (MDI), isophorone diisocyanate (IPDI), and 2,4-tolylene diisocyanate (TDI)] and short-chain diols (*e.g.*, butanediol, ethylene glycol, and propanediol) used as chain extenders, which can form strong hydrogen bonds and/or crystalline phases. The soft segments of TPUs usually consist of long polymeric chains of a macroglycol (polyether or polyester type), which are flexible and weakly polar. The difference in polarity and transition temperature between hard and soft segments can lead to the structural phase separation in the TPUs, which strongly influences the physical properties of resulting materials.[11] The physical and mechanical properties of TPUs depend on many factors such as the composition, length, sequence distribution, and topological structures (*e.g.*, branching and cross-linking) of both soft and hard segments.[12–14]

Since the hard segments act as the physical crosslinking between flexible chains, the crystallization of hard segments has a significant impact on the mechanical and processing properties of TPUs.[15–17] The thermal history of TPU would have a profound influence on the crystallization and viscoelastic properties of TPUs. Previous researchers have studied the order-disorder transition (ODT) and microphase separation transition (MST)[18–20] of TPUs. It is found that the crystallization of hard segments causes the ODT and MST process more complex. Although previous studies have investigated the relationships between the viscoelastic behavior of TPU and the crystallization of hard segments,[21–23] the dynamic viscoelastic responses of TPU during annealing treatment, which is of fundamental importance for 3D printing, have been seldom studied.

In this work, we investigated the dynamic viscoelastic properties of ester-based TPUs during the thermal annealing treatment under different conditions. The thermal annealing was

* Corresponding authors, E-mail: linglingni@zju.edu.cn (L.L.N.)
E-mail: panpengju@zju.edu.cn (P.J.P.)

Received May 9, 2024; Accepted August 12, 2024; Published online November 7, 2024

© Chinese Chemical Society
Institute of Chemistry, Chinese Academy of Sciences

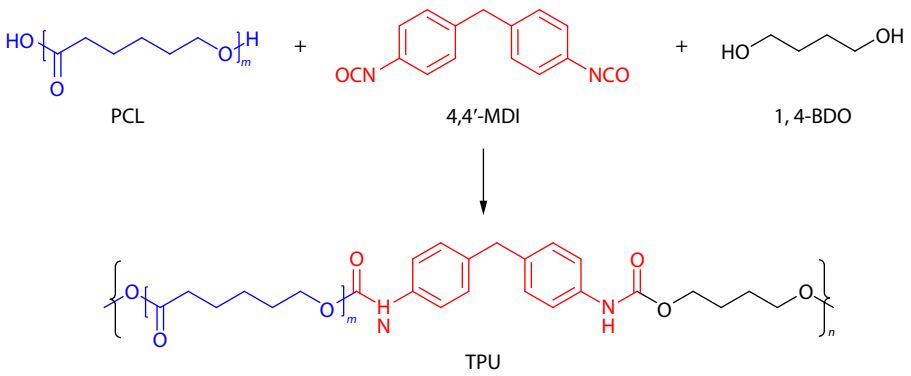

Fig. 1 Synthesis route to TPU.

conducted on a rotational-type rheometer with a parallel-plate fixture in an oscillatory mode. During the isothermal annealing process, we monitored the variations of dynamic storage and loss moduli (G' and G'') with time (t) and frequency (ω) of TPU with different hard segments contents. We found the obvious increases in G' and G'' in the isothermal dynamic time sweep experiments at a certain temperature region. The crystallites of hard segments grow up continuously during frequency scan (isothermal annealing treatment) and cause the extreme increase in G' and G'' with ω mainly in low ω region. For the TPUs with high content of hard segment, a complete high elastic platform with a width of three orders of magnitude was observed only through one frequency scan test at a certain temperature. We believe that this study would be essential for optimizing the physical performance of 3D-pirnted TPU products.

EXPERIMENTAL

Materials

Polycaprolactone diol (PCL-2000, M_n=2000 g/mol, Sinopharm Chem) was distilled under vacuum at 110 °C for purification. Diphenylmethane-4,4′-diisocyanate (MDI) and 1,4-butanediol (BDO) were purchased from Sinopharm Chemical Reagent Co., Ltd., China and dried by molecular sieves before use. Antioxygen 1010 was purchased from Ciba Guigy company, Swiss.

Preparation of TPU

To prepare the TPUs, PCL-2000 was added into a reaction vessel and heated to 80 °C, followed by the addition of melted MDI. After reaction for 3 h, BDO were added into the reaction mixture. Then the raw product was poured into a polytetrafluoroethylene dish and keep in 110 °C vacuum oven for 10 h. All the reactions were operated under N_2 environment (Fig. 1). To remove the thermal history before annealing measurement, all the obtained samples were hot-pressed at 190 °C after melting for 10 min, followed by slowly cooled to room temperature. The compression moulded samples were stored for at least a week at room temperature before the annealing experiments. The sample are cut to a wafer with 25 mm diameter and 1.7 mm thickness for the viscoelasticity test. The number-averaged molecular weight (M_n) and polydispersity index (PDI) of TPU with different hard segment contents are shown in Table 1. Fourier-transform infrared spectroscopy (FTIR) of TPU-30 was given in Fig. S1 (in the electronic supplementary information, ESI).

Table 1 Molecular weight and PDI of TPU with different hard segment content.

Sample	Hard segment content	M_n (g/mol)	PDI
TPU-25	24.3%	2.7×10^4	2.2
TPU-30	29.8%	3.0×10^4	2.1
TPU-40	40.9%	2.7×10^4	1.9

Characterization

Thermal transition behaviors of TPUs were measured on a Q100 differential scanning calorimetry (DSC, TA instruments, USA) under a N_2 atmosphere and a heating rate of 10 °C/min. The weight of sample was 5–10 mg for each measurement. The M_n and PDI was measured with a Waters 1515 GPC (Waters Co., Milford, MA) at 60 °C using dimethyl formamide (DMF) as the mobile phase (flow rate, 1.0 mL/min) and polystyrene as the standard for calibration.

FTIR spectra were measured on a Nicolet iS10 spectrometer (Thermo Fisher Scientific) equipped with an MCT detector at 32 scans and a resolution of 4 cm^{-1}.

Dynamic time and frequency sweep experiments were performed on a rheometer (ARES-G2, TA Instruments, USA) under N_2 flow using 25 mm diameter parallel plate geometry in an oscillatory mode. Antioxygen 1010 was added into TPU to avoid possible oxidization. Dynamic storage modulus (G') and loss modulus (G'') were measured as a function of angular frequency (ω) ranging from 0.03 rad/s to 100 rad/s at different temperatures (80–220 °C). A fixed strain of 1.0% was used at a given temperature, to ensure that measurements were taken well within the linear viscoelastic range of TPUs. Each sample was repeatedly measured for 3 times in the setting temperature. Dynamic time sweep experiments were conducted at various temperature with an ω=0.1 rad/s and a fixed strain of 1.0%.

RESULTS AND DISCUSSION

Effects of Isothermal Annealing on Thermal Behavior of TPU

DSC analysis was conducted to study the crystallization characteristics of hard segments in TPUs. Fig. 2 shows the DSC heating traces of TPU-30 samples after being annealed at the annealing temperature (T_a) of 100, 120, and 140 °C for different annealing time (t_a). The thermal transition at near −35 °C is attributed to the glass transition of PCL soft segments in original non-

https://doi.org/10.1007/s10118-024-3219-0

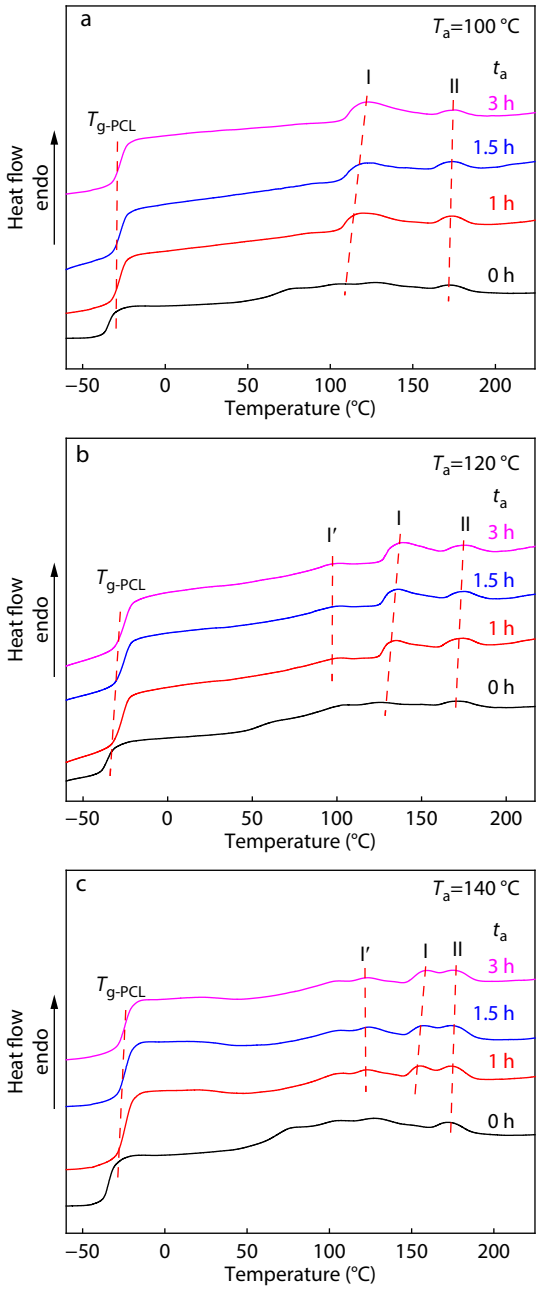

Fig. 2 DSC heating thermograms of TPU-30 sample after annealing at various T_a for different t_a: (a) T_a=100 °C; (b) T_a=120 °C; (c) T_a=140 °C.

annealed sample; the glass transition temperature (T_g) of PCL segment was denoted as $T_{g,PCL}$. The $T_{g,PCL}$ value moves to high temperature with increasing T_a or t_a. As the t_a is increased to 3 h, $T_{g,PCL}$ is shifted to −28 °C for the sample annealed at 100 °C, −28 °C for the sample annealed at 120 °C, and −25 °C for that annealed at 140 °C. These results clearly indicate that the degree of micro-phase separation became stronger with increasing annealing temperature.[24] In which, the formation of ordered hard domains experience hydrogen bonding association, crystal-like structure formation and size expansion processes.[25] High T_a and long t_a facilitate the formation of ordered hard domain, which could act as physical crosslinking points and retard the thermal movements of surrounded soft segments.

We note that the original non-annealed sample has two endotherms in the DSC heating curves, where the endotherm I locates at 110 °C and the endotherm II is at 173 °C. As the t_a is increased from 0 h to 3 h at 100 °C, endotherm I shifts to higher temperature and its peak area increases simultaneously (Fig. 2a). However, the peak temperature of endotherm II (denoted as T_m^{II}) and the corresponding peak area remains almost unchanged as t_a increases. These two endotherms are considered to be attributed to the melting of the crystallites of hard segment. The endotherm I and II are associated with the short-range and long-range ordering of hard segment domains, respectively.[26] Low T_a is not preferential for the formation of long-range of micro-crystallites with high melting point at *ca.* 173 °C. After annealed at 120 °C for 0.5–3 h, endotherm I moves to *ca.* 130 °C, yet endotherm II is still at *ca.* 173 °C (Fig. 2b). Furthermore, a new endothermic peak appears at ~100 °C (denoted as endotherm I′) after annealing at 120 °C, which is originated from the melt of shorter-range

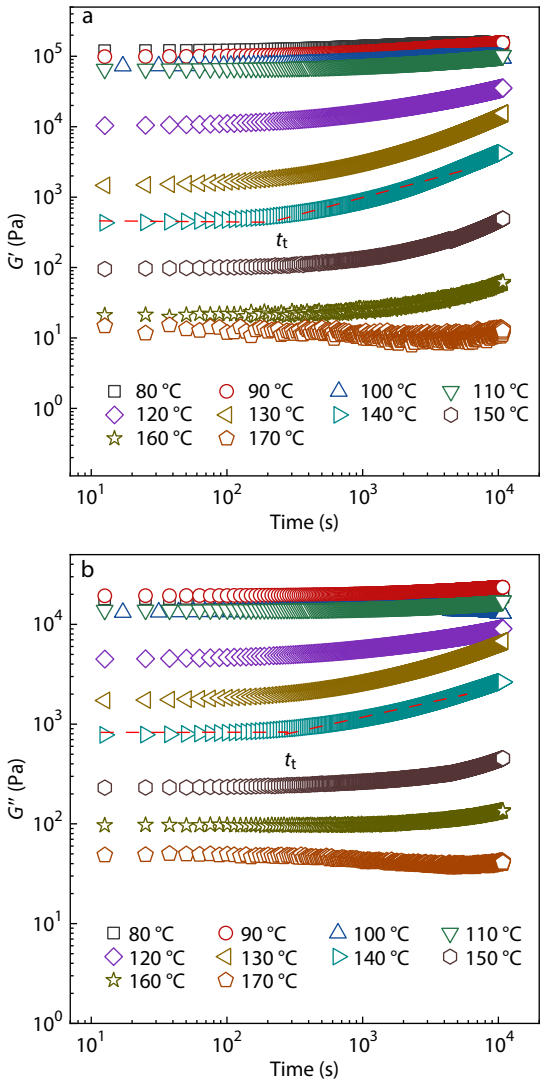

Fig. 3 Dynamic time sweep of TPU-30 at different annealing temperatures: (a) *G*′ curves; (b) *G*″ curves.

https://doi.org/10.1007/s10118-024-3219-0

hard domains ordered structure generated in secondary crystallization during long time annealing. However, the position of endotherm I′ ($T_m^{I'}$) hardly shifts with prolonging the t_a, since the T_a of 120 °C is higher than $T_m^{I'}$. While the T_a of 120 °C is slightly lower than the peak temperature of endotherm I (T_m^{I}). As the T_a increases to 140 °C, T_m^{I} and T_m^{II} are shifted to *ca*. 155 °C and 177 °C, with showing the small endotherm I′ at *ca*. 121 °C (Fig. 2c). The thermal annealing at different temperatures promote the crystallization of segments corresponding to endotherm I and II, rather than endotherm I′, resulting in the increase of T_m^{I} and T_m^{II} but not $T_m^{I'}$. The enhanced short-range, long-range and the new shorter-range of hard segments crystallites impose restriction on the movement of surrounds soft segments, thus leading to the increment of $T_{g,PCL}$ with increasing T_a and t_a.[27]

Effects of Isothermal Annealing on Dynamic Viscoelastic Behavior

Effects of thermal annealing on the dynamic viscoelastic parameters of TPU were further investigated. Fig. 3 shows the time evolutions of *G′* and *G″* for TPU-30 sample during isothermal annealing at 80–170 °C. At a certain temperature, *G′* and *G″* initially remain unchanged and then increase slowly with time for at least 150 min. At 170 °C, the values of *G′* and *G″* decreased slowly at the first 60 min and then increased slowly with time prolongs.

The transition time at which *G′* and *G″* begin to increase was denoted as t_t. The t_t of *G′* at different temperature is shown in Fig. 4(a). At the lower T_a (80–100 °C), the t_t of *G′* is as long as 1500 s. However, the t_t decreases sharply with the T_a increases to 110 °C. The shortest t_t is observed at the T_a of *ca*. 130 °C. The t_t increases again with further increasing T_a from 140 °C to 170 °C. When $t > t_t$, the slope of *G′* versus *t* at different T_a were calculated and are shown in Fig. 4(c). The slope initially increases slightly with T_a (T_a<120 °C) and goes through a maximum at T_a=130–140 °C. It then decreases and remains nearly unchanged with further increasing T_a to 160 °C. On the other hand, the t_t of *G″* at T_a<120 °C and T_a>160 °C is larger than the corresponding t_t values of *G′*, indicating that the growth of *G″* is slower than that of *G′* (Fig. 4b). However, at T_a = 130–140°C, the t_t of *G″* is almost the same as that of *G′*.

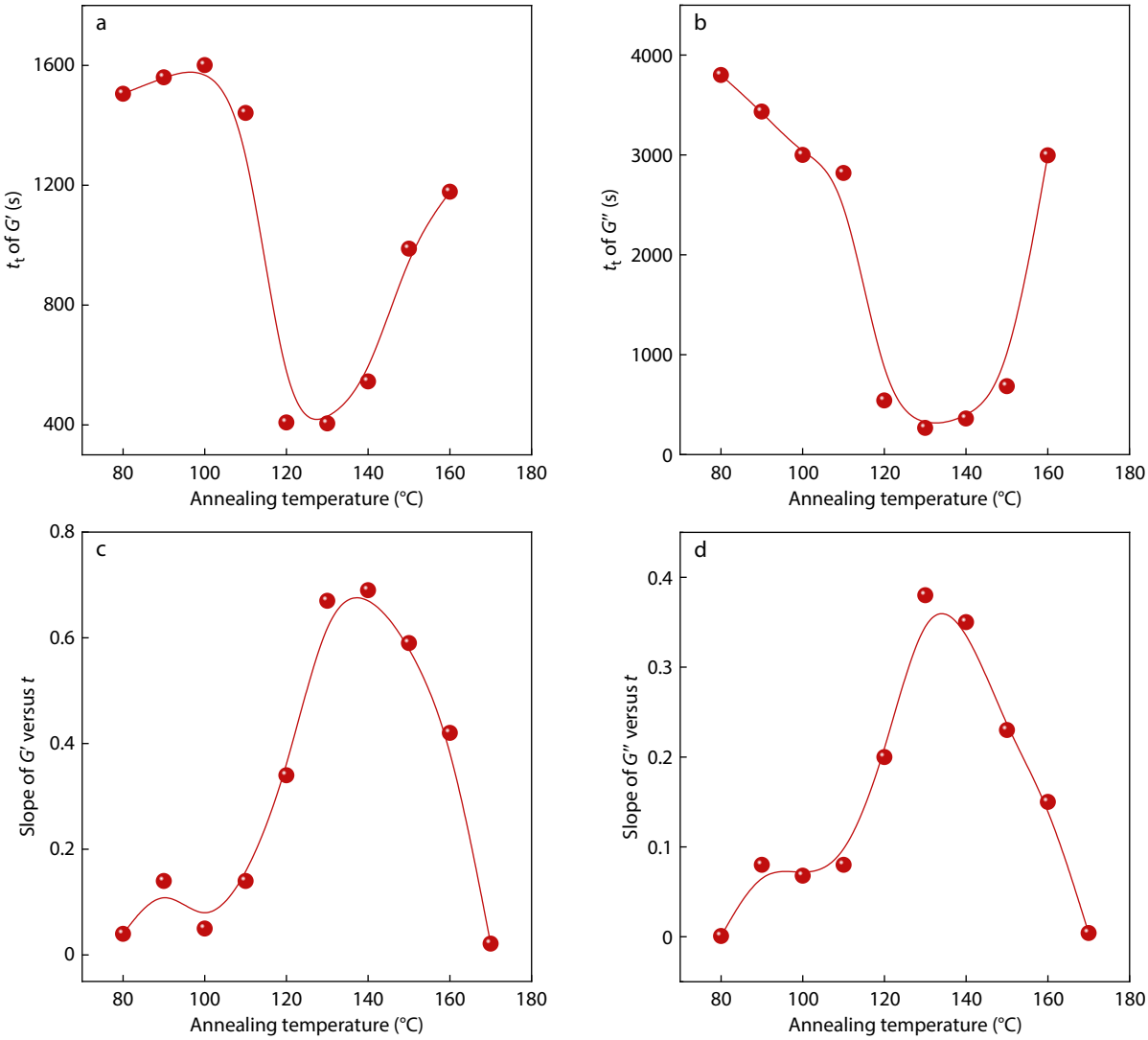

Fig. 4 t_t of (a) *G′* and (b) *G″*, the slope values of (c) *G′*~*t* and (d) *G″*~*t* after $t > t_t$ at different annealing temperatures for TPU-30.

https://doi.org/10.1007/s10118-024-3219-0

The slope of G'' versus t at $t > t_t$ also exhibits a similar evolution trend as that of G' (Fig. 4d), but the value of slope is smaller than that of G', implying that the G'' increases slowly than G' at $t > t_t$.

In essence, the slope of G' versus t reflects the crystallization rate of hard segments in TPU during the annealing process. The T_m^I value of TPU shown in Fig. 2(a) is about 120 °C, and its temperature corresponding to the maximum crystallization rate (T_{max}) is *ca.* 100 °C. The t_t of G' at 100 °C is about 1600 s, which is close to 0.5 h. With the t_a further prolongs, the endotherm I shown in Fig. 2(a) are enhanced. However, the extremely small slope (0.06) at $t > t_t$ demonstrates the slight increase of G' of TPU-30, corresponding to the slight shift of T_m^I to high temperature (Fig. 2a). This reveals that the isothermal annealing at 100 °C could only promote the crystallization of hard segments to form smaller crystallites.

As shown in Fig. 4(c), the slope of G'~t exhibits the highest value at T_a=130–150 °C, which is near the T_{max} values of both T_m^I and T_m^{II} but higher than $T_m^{I'}$ (Fig. 2c). Within this temperature range, the movability of medium-length hard segments would be strengthened and easy to form more perfect and larger crystallites. With the time evolving, more and more crystallites are generated and acted as crosslinking point, causing a significant increase in G' for at least 3 h. With T_a further increases to 170 °C, the slopes of G'~t become small again. At high T_a, the thermal motion of chain segments and melting of crystallites dominate the annealing process, leading to the slow decreases of G' and G''. At lower T_a (80–110 °C), G' is always larger than G'' and the elasticity dominates (Fig. 3). At T_a=130–150 °C, G'' is larger than G' initially and then G' is higher than G'' at the end of annealing treatment, meaning that the annealing enhances mainly the elastic component. At higher T_a (160–170 °C), G'' is always hither than G' in the annealing process. Therefore, to achieve high modulus for TPU, it is better to anneal at a medium T_a region of 130–150 °C for a certain time (*e.g.*, $t > t_t$).

Based on the results shown in Fig. 3, the relationship between G', G'' and temperature at different t_a can be evaluated, as shown in Figs. 5(a) and 5(b). At the same t_a, both G' and G'' decrease with temperature. At low (<120 °C) and high (>160

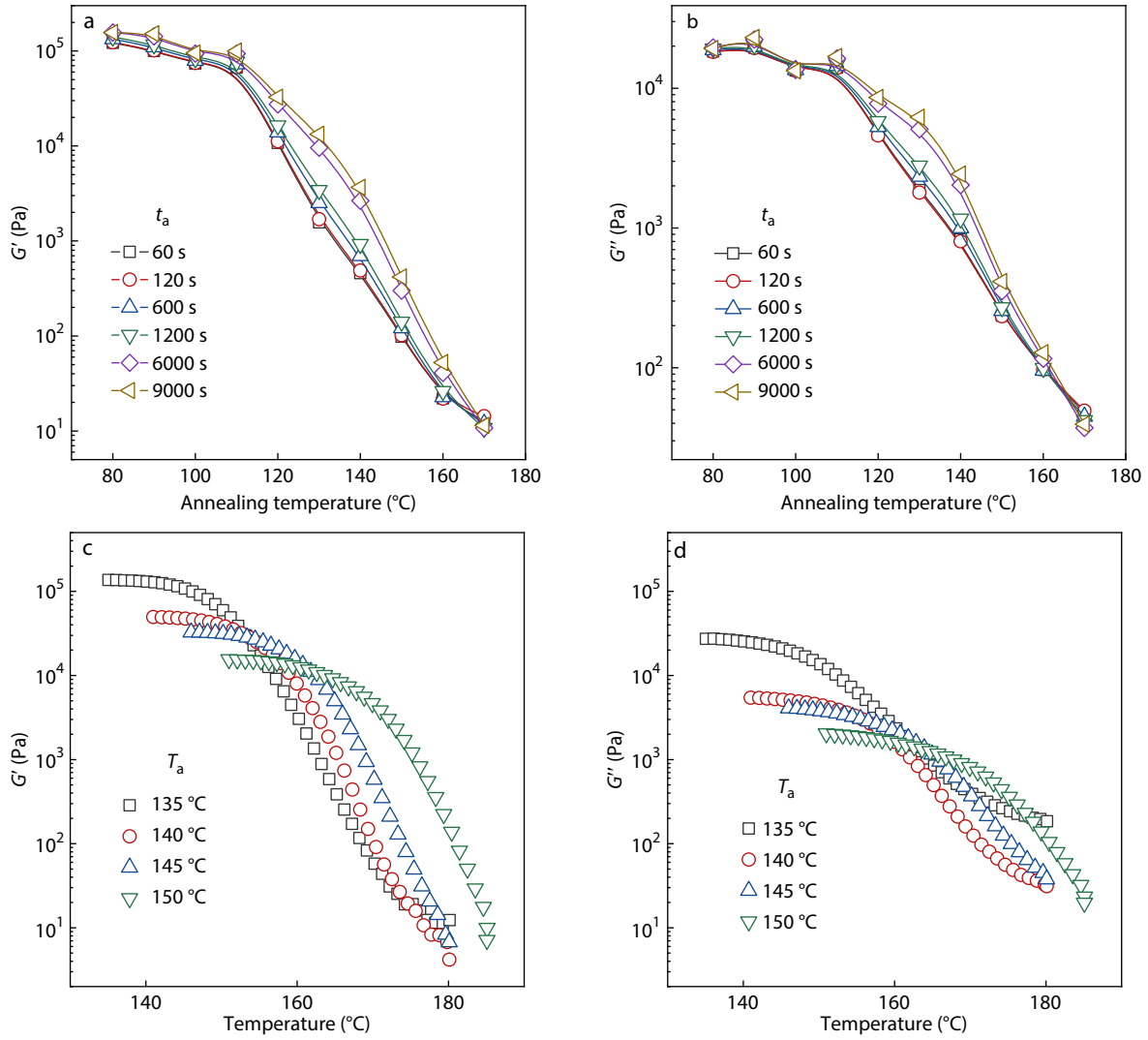

Fig. 5 (a, b) Changes of (a) G' and (b) G'' with annealing temperature for TPU-30 after being annealed for various annealing time. (c) Temperature scan test of TPU-30 after being annealed at different annealing temperatures for 5 h.

https://doi.org/10.1007/s10118-024-3219-0

°C) temperature, the G' and G'' remain nearly unchanged with t_a increases. However, both G' and G'' increase with t_a at T_a=120–150 °C, leading to the rise of transition temperature. In another experiment, the TPU was heated to 180 °C for 10 min to eliminate the heat history, and was then cooled at a rate of 30 °C/min to the corresponding T_a (135, 140, 145, and 150 °C) for 5 h annealing. Afterwards, the temperature scan tests were conducted on these samples. Figs. 5(c) and 5(d) shows that the sample is elastic at the annealing temperature of 135–150 °C and the transition temperature rises with the increase of T_a. Note that the T_a range of 135–150 °C locates in the region with high slope value, as shown in Figs. 4(c) and 4(d). The molecular chains have higher mobility and produce more perfect crystals at higher T_a, resulting in the higher transition temperature.

Frequency Dependence of Dynamic Viscoelastic Parameters under Annealing

Since the T_a and t_a have pronounced influences on viscoelastic behavior, G' and G'' of TPU-30 under different angular frequency (ω) were further investigated. Fig. 6 shows the repeated dynamic frequency sweeps for TPU-30 at different temperature. At T_a=110 °C, G' is always larger than G'' over the measured ω scope (Fig. 6a), which is the characteristic of crosslinked network. The value of G' enhances slightly with the measurement times. The increment of G' is more obvious in lower ω region than that in higher ω region. G'' has almost the same value during the three measurements. The increment of G' with measurement times is enhanced as T_a increases from 120 °C to 140 °C, especially in the lower ω region (Figs. 6b–6d).

As T_a further increases to 150 and 160 °C, G' does not scale up with measurement times as that observed at lower temperature (Figs. 6e and 6f). At T_a=120–150 °C, there is an intersection between G' and G'' curves, where the corresponding angular frequency is denoted as ω_i. Different from the typical rheological characteristics of polymer melts, G' is smaller than G'' at higher ω region ($\omega>\omega_i$), while G' is larger than G'' at lower ω region ($\omega<\omega_i$). The ω_i shifts to higher ω with increasing the measurement time. This is considered to be caused by the crystallization of hard segments during measurement at a fixed temperature (or the isothermal annealing process). The crystallization of hard segments primarily enhances the G' value and lead ω_i to shift towards high ω. We can observe the obvious increment of G' in low ω region, while the increments are relatively small in high ω region at T_a=120–150 °C. This demonstrates that the crystallization of hard segment during thermal annealing restrains the relaxation of motion units with relatively large size (low ω region), but hardly influences the relaxation of units with small size (high ω region). G' is not sensitive to ω and shows a plateau at low ω region, this is attributed to the existence of network structure with the ordered hard domains as crosslinking point, as reported previously.[19] At T_a=160 °C, ω_i disappears and G'' is larger than G' over the entire range of measured frequency, behaving as a

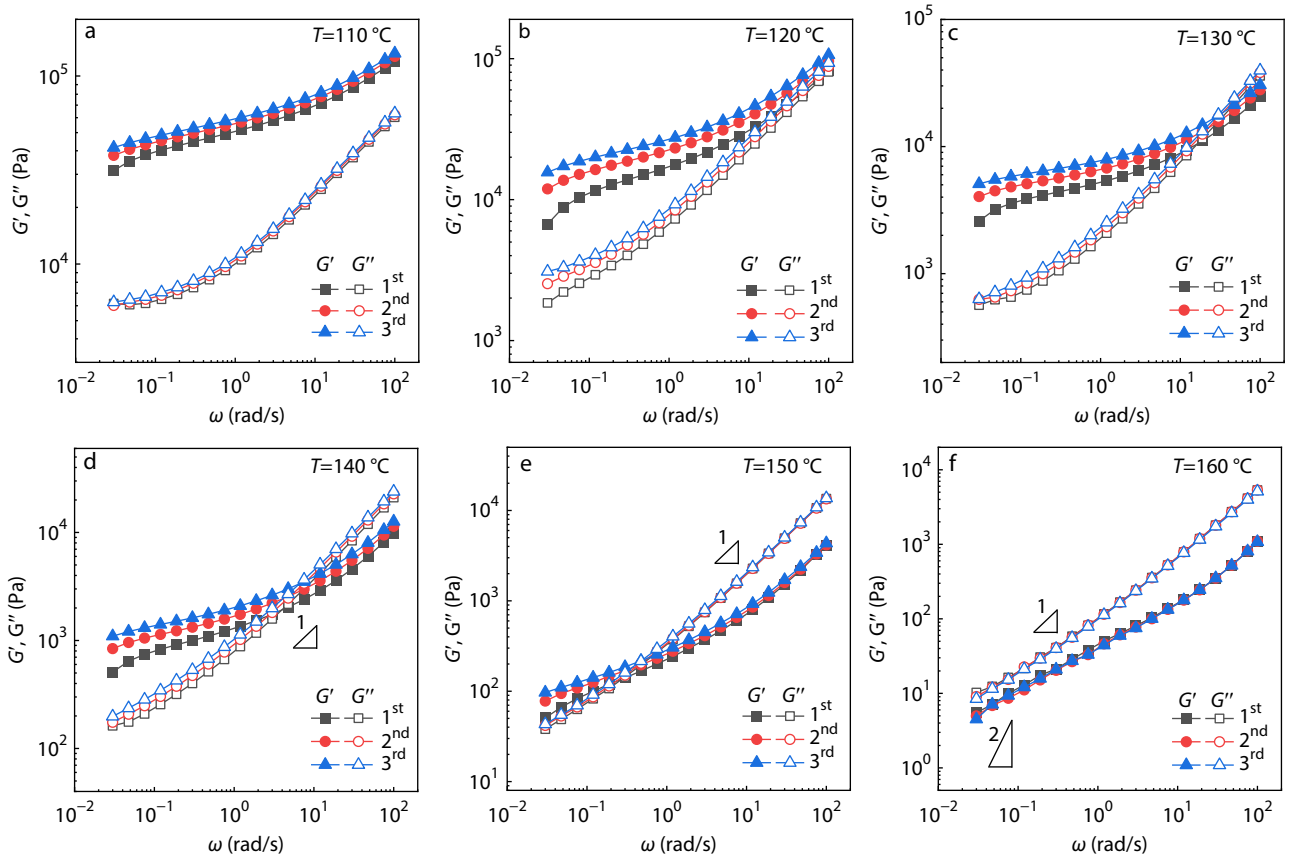

Fig. 6 Repeating dynamic frequency sweeps with three times for TPU-30 at different annealing temperature: (a) 110 °C; (b) 120 °C; (c) 130 °C; (d) 140 °C; (e) 150 °C; (f) 160 °C.

https://doi.org/10.1007/s10118-024-3219-0

polymer melt (Fig. 6f). The G'' is almost proportional to the ω, *i.e.*, $\log G'' \propto \log\omega$; this indicates that the dynamic viscosity is not greatly affected by the angular frequency. However, the viscoelastic properties are not in the Newtonian region because the scale relation of $\log G' \propto 2\log\omega$ is not found in lower ω region, probably arousing from the hydrogen bonding interactions between hard segments. For TPU-30, ω_i only appears at T_a=120–155 °C. The reciprocal of ω_i is denoted as τ_i.

Fig. 7 shows the evolution of τ_i (derived from ω_i at the first measurement) with T_a, in which τ_i increases with T_a, which is similar to the polymer systems with hydrogen bonding.[28] At higher T_a, the micro-crystalline domains may restrain the movement of unit with larger size, leading to a long relaxation time.

According to the classical theory of rubber elasticity,[29] the average molecular weight between neighboring crosslink points (M_c) can be calculated using the plateau modulus (G_p) by $M_c = \rho RT/G_p$, where ρ is the polymer density and R is the ideal gas constant, T is the Kelvin temperature. The polymer density at 120–150 °C is approximately 1000 kg/m^3 and G_p is determined from the plateau. The evaluated M_c at different T_a is shown in Table 2. With increasing T_a, the crystalline domains gradually melts, leading to an increase of M_c. The M_n of TPU-30 is 3.1×10^4 g/mol. The larger value of M_c than M_n implies that the chain length between neighboring crosslinked points contains several TPU chains, in which the TPU chains may connect together through the ordered hard domains between hard segments.

Effects of Hard Segment Content on the Dynamic Viscoelastic Parameters of TPU

The frequency evolution of dynamic viscoelastic parameters for TPUs with different contents of hard segments were investigated at various T_a. Figs. 8(a)–8(e) and Fig. S2 (in ESI) show the variation of G' and G'' with ω at various T_a for TPU-25. Similar to TPU-30, the almost same curves are observed in the three frequency scan measurements at both low (70, 80 °C) and high (130, 140 °C) T_a, but different curves are observed at moderate T_a (90–120 °C), where the values of G' at various ω (especially in low ω region) increase with the measurement times. There is an intersection point between G' and G'' curves within 30 °C (from 90 °C to 120 °C), which is 40 °C (from 120 °C to 160 °C) for TPU-30. The difference was aroused by the decrease of hard segment content that can act as crosslinking point (Fig. 8f). Likewise, the amplification of G' of TPU-25 with measurement times in low ω region was not so obvious as that for TPU-30. At high T_a (140 °C, Fig. 8e), the scale relation of $\log G'' \propto 2\log\omega$ in lower ω region is also not observed for TPU-25.

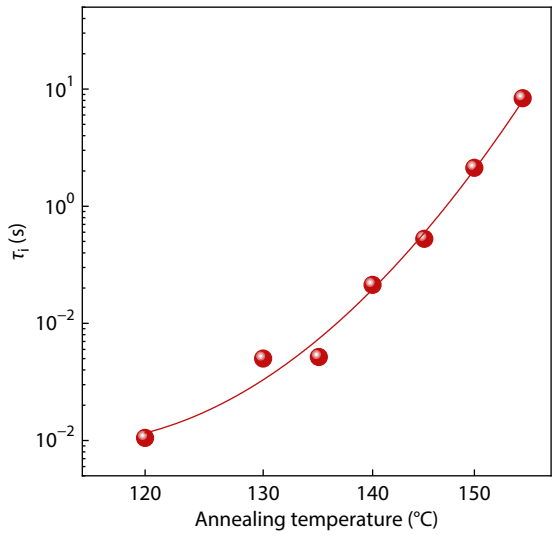

Fig. 7 Evolution of τ_i with annealing temperature for TPU-30. τ_i is derived from the frequency (ω_i) corresponding to the intersection of G' and G'' at the first measurement.

Table 2 M_c of TPU-30 at different annealing temperatures.

T_a (°C)	120	130	140	150
M_c	2.9×10^4	1.9×10^5	9.6×10^5	1.5×10^6

Fig. 9 and Fig. S3 (in ESI) show the variations of G' and G'' with ω at various T_a for TPU-40. The measurable T_a region was much higher than that of TPU-25 and TPU-30, due to the high content of hard segments. Fig. S4 (in ESI) gives the DSC curves of pure hard segments with three melting peaks located at 160, 210 and 226 °C, respectively. At T_a=170 °C, both G' and G'' increase evidently with the measurement time in lower ω region, but no intersection point appears between G' and G'' (Fig. 9a). When the T_a increases to 180 °C, an intersection point between G' and G'' emerges (Fig. 9b). Interestingly, two intersection points was observed at the first measurement. Similar to TPU-30, the intersection point in higher ω region is regarded as ω_i, which is the reciprocal of Rouse time for mesh chains.[30] The intersection point in lower ω region is regarded as the reciprocal of the relaxation time (τ_{rel}) of a TPU chain in network structure, *i.e.*, ω_{rel}. The region between ω_{rel} and ω_i was thus considered as the high elastic platform, in which G' is insensitive to ω. At the second and third measurements, ω_i increases from 0.3 to 7.5 and 100, respectively; meanwhile, ω_{rel} shfits toward low ω and could not be observed over the tested frequency range. Nonetheless, we could speculate the ω_{rel} at the second measurement should be lower than that at the first measurement according to Fig. 9, indicating that the high elastic platform is widened with increasing measurement times.

As the T_a increases further, the increment of G' and G'' becomes more obvious with the measurement time. The decomposition temperature of TPU-40 is *ca.* 260 °C. In order to avoid the possible thermal oxidation, the highest temperature tested is set to be 220 °C. Both ω_i and ω_{rel} could be observed at T_a=180–220 °C (Figs. 9b–9f). Different from TPU-25 and TPU-30, $G'' > G'$ is not observed over the entire measured frequency range for TPU-40 at high T_a. The ω_i and ω_{rel} values evaluated at different T_a and measurement times are summed in Table S1 (in ESI). We note that ω_{rel} shifts towards lower ω, but ω_i shifts towards higher ω with increasing the measurement times at T_a=180–220 °C. It is considered that isothermal annealing treatment could widen the high elastic platform by promoting the crystallization of hard segments at moderate temperature.

According to $\omega_i \approx \dfrac{KT}{\zeta b^2 N_i^2}$, the increased crystallites can shorten the mesh chains (N_i), leading to the decrease of Rouse time and increase of ω_i. The annealing treatment at moder-

https://doi.org/10.1007/s10118-024-3219-0

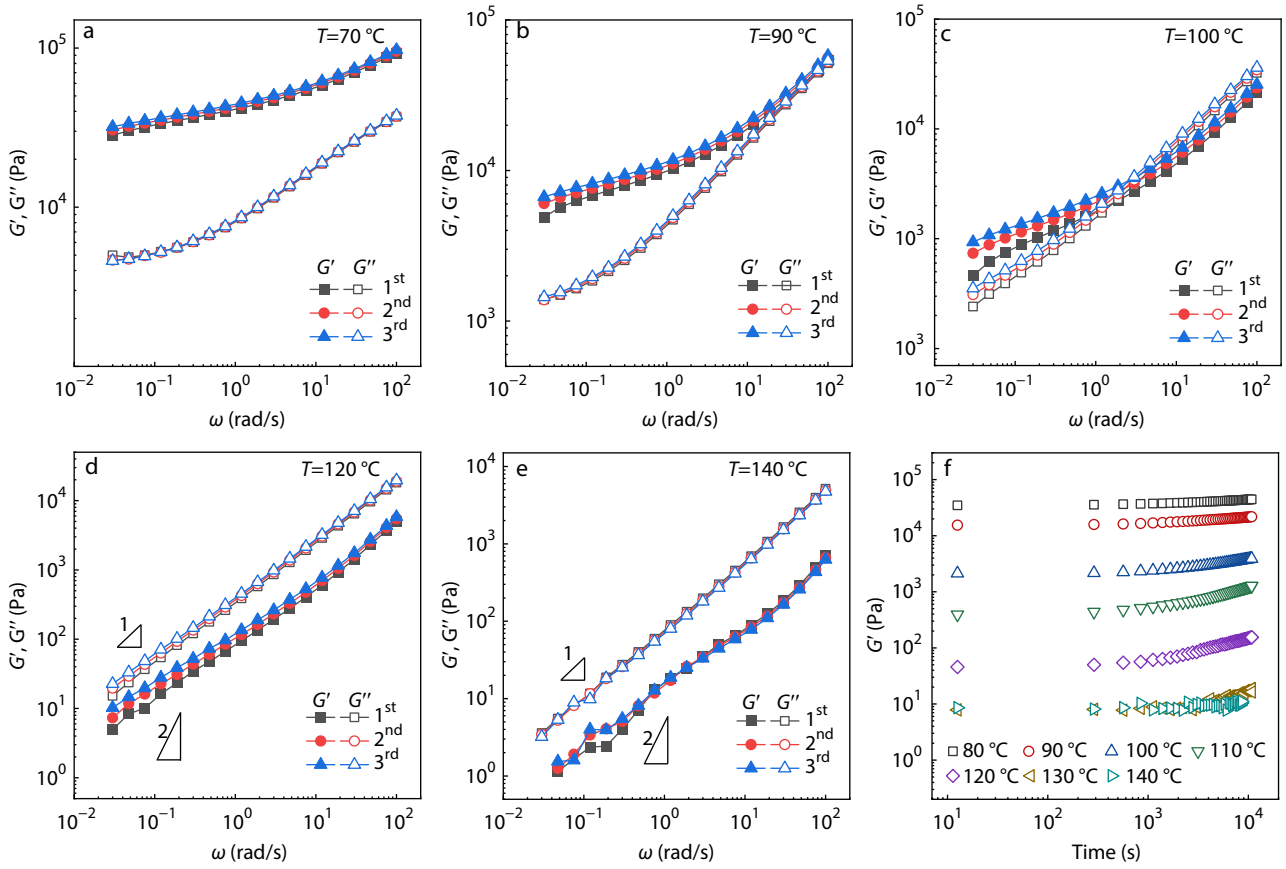

Fig. 8 (a–e) Repeating dynamic frequency sweeps with three times for TPU-25 at different annealing temperatures: (a) 70 °C; (b) 90 °C; (c) 100 °C; (d) 120 °C; (e) 140 °C. (f) Dynamic time sweeps for TPU-25 at different annealing temperatures.

ate T_a enhances the crystallization of hard segments (acting as the physical crosslinking points), which can widen the high elasticity platform through the decrease of ω_{rel} and the increase ω_i. The M_c values of TPU-25 and TPU-40 at different T_a was calculated and shown in Table 3 and Table 4. Similar as TPU-30, $M_c \geq M_n$ is observed for both TPU-25 and TPU-40, implying that the chain length between neighbouring crosslinking points contains several TPU chains bonded through the ordered hard domains between hard segments.

Furthermore, the region between ω_i and ω_{rel} is also widened with increasing T_a. The high elastic platform become obvious and typically located at 210–220 °C for TPU-40. We note that the width of high elasticity plateaus at 210 and 220 °C are only 3 orders of magnitude, much narrower than that of typical linear polymers (6–9 orders of magnitude).[31] A complete high elastic platform is usually observed in a master curve through time-temperature superposition. Herein, the complete high elastic platform was only observed through one frequency scan test at a certain temperature. Of course, the width between ω_i and ω_{rel} was also affected by T_a. As mentioned above, the width of high elastic platform at T_a=210 and 220 °C are only 3 orders of magnitude for TPU-40, implying that only a small portion of hard segment crystallites acted as the crosslinking points at high T_a.

We note that both G' and G'' of TPU-40 decrease sharply in lower ω region with the ω decreasing, which differs from TPU-25 and TPU-30 and also differs from the classic linear viscoelasticity theory.[32] The slopes of log G' and log G'' versus log ω are respectively 2.0 and 3.7 at 210 °C, 3.9 and 3.0 at 220 °C (Figs. 9e and 9f). As described in Experimental section, the frequency scan test was carried out from low ω to high ω region. The measurement at low ω usually spends longer time than that at high ω. For example, it took 15 mins for the data point measured at ω=0.03 rad/s and only 2 min at ω=30 rad/s. As mentioned above, the measurement process is actually an annealing treatment. During the measurement, the crystallites of hard segments can grow continuously, which causes the increase in G' and G'' with ω increasing and leads to the high slope in lower ω region.

CONCLUSIONS

In this work, we have investigated the viscoelastic properties and evolutions of TPU with different hard segment content during thermal annealing at different temperature. The results show that the G' of TPU-30 has an increment over time only at a moderate T_a range, which corresponds to the temperature with the fastest crystallization rate of hard segments. However, G' remains nearly unchanged with time at both high or low T_a. The growth of G'' over time is smaller than that of G'. At moderate T_a, both G' and G'' increase during the repeating frequency sweep, especially in lower ω region, due to the gradually enhanced crystallization of hard segments. When the content of hard segment in TPU is decreased, the increment of G' and G'' are weak-

https://doi.org/10.1007/s10118-024-3219-0

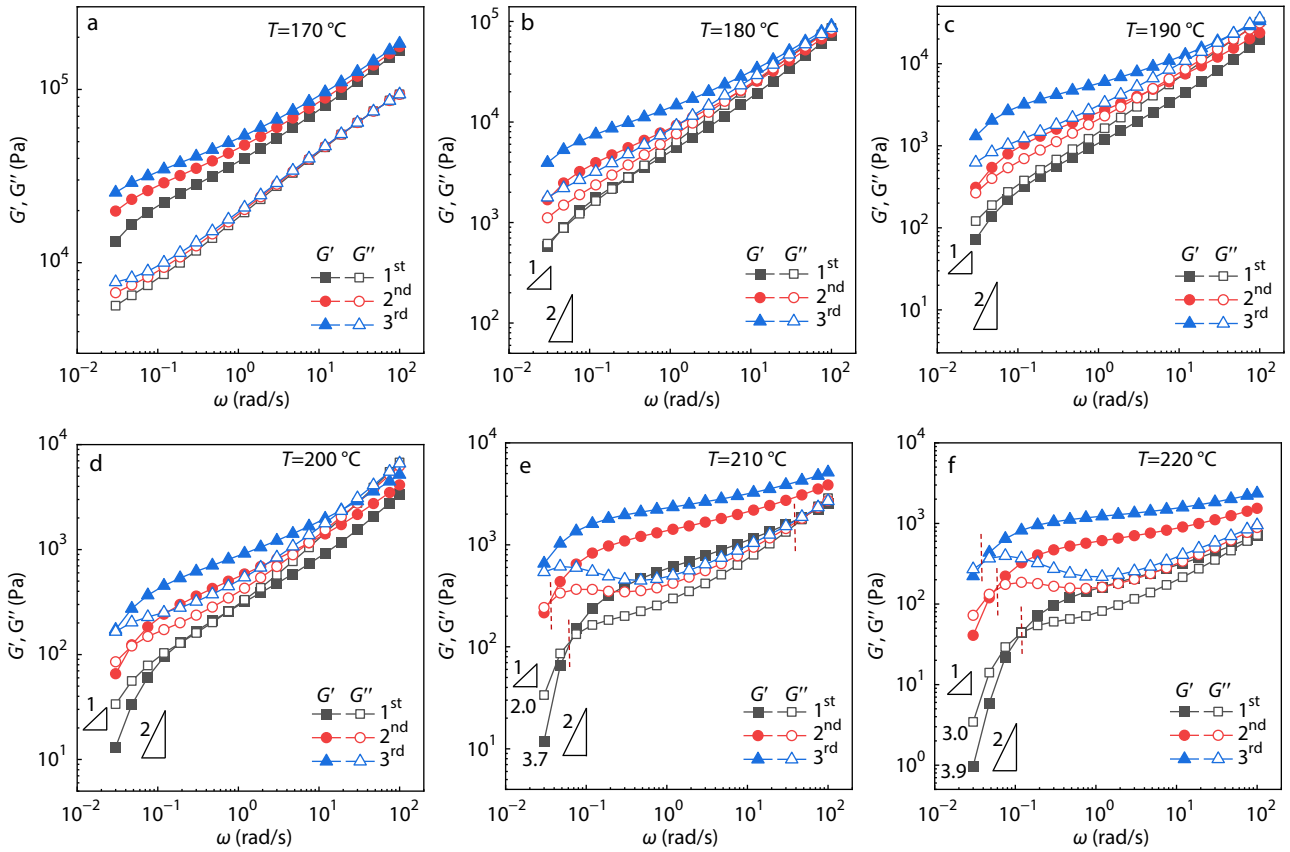

Fig. 9 Repeating dynamic frequency sweeps with three times for TPU-40 at different annealing temperatures: (a) 170 °C; (b) 180 °C; (c) 190 °C; (d) 200 °C; (e) 210 °C; (f) 220 °C.

Table 3 M_c of TPU-25 at different annealing temperatures.

T_a (°C)	70	80	90	100	110
M_c of TPU-25 (g/mol)	6.6×10^4	5.0×10^4	3.4×10^5	1.6×10^6	1.8×10^6

Table 4 M_c of TPU-40 at different annealing temperatures.

T_a (°C)	160	170	180	190	200	210	220
M_c of TPU-40 (g/mol)	2.4×10^4	7.4×10^4	2.8×10^5	6.1×10^5	4.4×10^6	1.6×10^6	3.1×10^6

ened. For TPU-40, a complete high elastic platform with a width of 3 orders of magnitude was observed through one frequency scan test at a certain temperature. In addition, the crystallites of hard segments grow up continuously during the frequency scan test (or isothermal annealing treatment), causing the high slope of G'~ω and G''~ω curves in low ω region. The results obtained in this study would be crucial for the processing of TPU materials.

Conflict of Interests

The authors declare no interest conflict.

Electronic Supplementary Information

Electronic supplementary information (ESI) is available free of charge in the online version of this article at http://doi.org/10.1007/s10118-024-3219-0.

Data Availability Statement

The data that support the findings of this study are available from the corresponding author upon reasonable request. The author's contact information: panpengju@zju.edu.cn.

REFERENCES

1 Martin, D. J.; Osman, A. F.; Andriani, Y.; Edwards, G. A. Thermoplastic polyurethane (TPU)-based polymer nanocomposites. *Adv. Polym. Nanocompos.* **2012**, 321–350.

2 Amjed, N.; Bhatti, I. A.; Simon L.; Castel, C. D.; Zia, K. M.; Zuber, M.; Hafiz, I.; Murtaza, M. A. Preparation and characterization of thermoplastic polyurethanes blended with chitosan and starch processed through extrusion. *Int. J. Biol. Macromol.* **2022**, *208*, 37–44.

3 Abdul Halim, N. H. A.; Amin, K. N. M. Rheological properties of cellulose nanocrystals isolated *via* mechanical methods in thermoplastic polyurethane matrix. *Mater. Today: Proc.* **2022**, *57*, 1021–1026.
4 Zhang, Q. Y.; Huang, K.; Tan, J.; Lei, X. X.; Huang, L. P.; Song, Y. T.; Li, Q. J.; Zou, C. Y.; Xie, H. Q. Metal-phenolic networks modified polyurethane as periosteum for bone regeneration. *Chin. Chem. Lett.* **2022**, *33*, 1623–1626.
5 Chennell, P.; Feschet-Chassot, E.; Sautou, V.; Mailhot-Jensen, B. Preparation of ordered mesoporous and macroporous thermoplastic polyurethane surfaces for potential medical applications. *J. Biomater. Appl.* **2018**, *32*, 1317–1328.
6 Liu, C.; Yang, D.; Sun, M. N.; Deng, G. J.; Jing, B. H.; Wang, K.; Shi, Y. Q.; Fu, L. B.; Feng, Y. Z.; Lv, Y. C.; Liu, M. H. Phosphorous-Nitrogen flame retardants engineering MXene towards highly fire safe thermoplastic polyurethane. *Compos. Commun.* **2022**, *29*, 101055.
7 Martin, D. J.; Warren, L. A. P.; Gunatillake, P. A.; McCarthy, S. J.; Meijs, G. F.; Schindhelm, K. Polydimethylsiloxane/polyether mixed macrodiol-based polyurethane elastomers: biostability. *Biomaterials* **2000**, *21*, 1021–1029.
8 Guo, J. Z.; Chen, Y. F.; Zhang, P.; Li, G.; Yang, X. N.; Wang, C. F.; Chen, S. Easy-to-perform organic-solvent-free synthesis of carbon dots with strong green photoluminescence. *Chin. Chem. Lett.* **2024**, *35*, 108481.
9 Yilgör, I.; Yilgör, E.; Wilkes, G. L. Critical parameters in designing segmented polyurethanes and their effect on morphology and properties: a comprehensive review. *Polymer* **2015**, *58*, A1–A36.
10 Backes, E. H.; Harb, S. V.; Pinto, L. A.; Moura, N. K.; Morgado, G. F.; Marini, J.; Passador, F. R.; Pessan, L. A. Thermoplastic polyurethanes: synthesis, fabrication techniques, blends, composites, and applications. *J. Mater. Sci.* **2024**, *59*, 1123–1152.
11 Wang, H. R.; Litvinov, V.; Yu, W.; Peh, K. W. E.; Yu, Q. L.; Men, Y. F. Temperature-induced evolution of micro-structure and chain dynamics in thermoplastic polyurethane with low hard segment content as studied by *in situ* synchrotron SAXS and time-domain NMR experiments. *Chinese J. Polym. Sci.* **2023**, *41*, 1902–1911.
12 Nichetti, D.; Grizzuti, N. Determination of the phase transition behavior of thermoplastic polyurethanes from coupled rheology/DSC measurements. *Polym. Eng. Sci.* **2004**, *44*, 1514–1521.
13 Velankar, S.; Cooper, S. L. Microphase separation and rheological properties of polyurethane melts. 2. Effect of block incompatibility on the microstructure. *Macromolecules* **2000**, *33*, 382–394.
14 Yilgör, E.; Yilgör, İ. Influence of soft segment structure, hydrogen bonding, and diisocyanate symmetry on morphology and properties of segmented thermoplastic polyurethanes and polyureas. *Turk. J. Chem.* **2023**, *47*, 1007–1017.
15 Yoon, P. J.; Han, C. D. Effect of thermal history on the rheological behavior of thermoplastic polyurethanes. *Macromolecules* **2000**, 33, 2171–2183.
16 Lee, K. M.; Han, C. D. Microphase separation transition and rheology of side-chain liquid-crystalline block copolymers. *Macromolecules* **2002**, *35*, 3145–3156.
17 Gao, Z. D.; Wang, Z. Y.; Liu, Z. R.; Fu, L. L.; Li, X. K.; Eling, B.; Poselt, E.; Schander, E.; Wang, Z. B. Hard block length distribution of thermoplastic polyurethane determined by polymerization-induced phase separation. *Polymer* **2022**, *256*, 125236.
18 Yuan, Q.; Zhou, T.; Li, L.; Zhang, J. H.; Liu, X. F.; Ke, X. L.; Zhang, A. M. Hydrogen bond breaking of TPU upon heating: understanding from the viewpoints of molecular movements and enthalpy. *RSC Adv.* **2015**, *5*, 31153–31165.
19 Jouibari, I. S.; Haddadi-Asl, V.; Ahmadi, H.; Mirhosseini, M. M. Micro-phase separation kinetics of polyurethane nanocomposites with neural network. *Polym. Compos.* **2019**, *40*, 3904–3913.
20 Cossar, S.; Nichetti, D.; Grizzuti, N. A rheological study of the phase transition in thermoplastic polyurethanes. Critical gel behavior and microstructure development. *J. Rheol.* **2004**, *48*, 691–703.
21 Mirhosseini, M. M.; Haddadi-Asl, V.; Jouibari, I. S. How the soft segment arrangement influences the microphase separation kinetics and mechanical properties of polyurethane block polymers. *Mater. Res. Exp.* **2019**, *6*, 085311.
22 Zeng, Y.; Chen, Y. Z.; Sha, D.; Wu, Y. C.; Qiu, R. H.; Liu, W. D. Highly stretchable fatty acid chain-dangled thermoplastic polyurethane elastomers enabled by H-bonds and molecular chain entanglements. *ACS Sustainable Chem. Eng.* **2022**, *10*, 11524–11532.
23 Kojio, K.; Furukawa, M.; Nonaka, Y.; Nakamura, S. Control of mechanical properties of thermoplastic polyurethane elastomers by restriction of crystallization of soft segment. *Materials* **2010**, *3*, 5097–5110.
24 Yamasaki, S.; Nishiguchi, D.; Kojio, K.; Furukawa, M. Effects of aggregation structure on rheological properties of thermoplastic polyurethanes. *Polymer* **2007**, *48*, 4793–4803
25 Kong, Z. Y.; Ying, W. B.; Hu, H.; Wang, K.; Chen, C.; Tian, Y.; Li, F. L.; Zhang, R. Y. Formation of crystal-like structure and effective hard domain in a thermoplastic polyurethane. *Polymer* **2020**, *210*, 123012.
26 Valim, F. C. F.; Oliveira, G. P.; da Cunha Vasconcelos, G.; de Paiva, L. B.; Santillo, C.; Lavorgna, M.; Andrade, R. J. E. Unraveling the impact of phase separation induced by thermal annealing on shape memory effect of polyester-based thermoplastic polyurethane. *J. Appl. Polym. Sci.* **2022**, *139*, e51723.
27 Hesketh, T. R.; Van Bogart, J. W. C.; Cooper, S. L. Differential scanning calorimetry analysis of morphological changes in segmented elastomers. *Polym. Eng. Sci.* **1980**, *20*, 190–197.
28 Saari, R. A.; Maeno, R.; Tsuyuguchi, R.; Marujiwat, W.; Phulkerd, P.; Yamaguchi, M. Impact of lithium halides on rheological properties of aqueous solution of poly(vinyl alcohol). *J. Polym. Res.* **2020**, *27*, 218.
29 Treloar, L. R. G. The Physics of Rubber Elasticity, 3rd Ed., Oxford University Press, **1975**.
30 Ni, Q. S.; Ye, W. J.; Du, M.; Shan, G. R.; Song, Y. H.; Zheng, Q. Effect of hydrogen bonding on dynamic rheological behavior of PVA solution. *Gels* **2022**, *8*, 518.
31 Colby, R.; Fetters, L.; Graessley, W. The melt viscosity-molecular weight relationship for linear polymers. *Macromolecules* **1987**, *20*, 2226–2237.
32 Rubinstein, M.; Colby, R. *Polymer Physics*, Oxford University Press, **2003**.

https://doi.org/10.1007/s10118-024-3219-0